Space- and time-resolved density measurements of a high-intensity laser-produced plasma for x-ray laser studies

S. Dobosz, P. D'Oliveira, S. Hulin, P. Monot, F. Réau, and T. Auguste
Commissariat à l'Energie Atomique, DSM/DRECAM/SPAM, C.E. Saclay, 91191 Gif-sur-Yvette Cédex, France
(Received 8 November 2001; published 5 April 2002)

We present a detailed study on the spatiotemporal density evolution of a plasma created by optical-field ionization of a high-pressure pulsed gas jet by a 10-TW, 60-fs Ti:sapphire laser. The plasma dynamics has been studied on a 17-ns time scale with a 60-fs time resolution and a 5-μm space resolution using a Mach-Zehnder interferometer. The density profile and the plasma radial expansion were accurately measured for conditions relevant to x-ray laser schemes in H-like nitrogen which were recently proposed [S. Hulin *et al.*, Phys. Rev. E **61**, 5693 (2000)]. The results were reproduced well by hydrocode simulations that allowed to infer the plasma temperature.

DOI: 10.1103/PhysRevE.65.047403 PACS number(s): 52.50.Jm, 52.35.Mw, 52.25.Os

With the development of table-top terawatt lasers, new x-ray laser schemes based on the rapid recombination following optical-field ionization (OFI) of a gas by a short-pulse high-intensity laser have been proposed. Lasing in H-like Li at 135 Å has already been reported by several laboratories [1]. Calculations show that dense and cold plasmas are required to obtain suitable conditions for lasing [2]. On the other hand, measurements performed on optically ionized gases have demonstrated that the plasma electron temperature is driven by above threshold ionization (ATI) for moderate densities (10^{16}–10^{18} cm^{-3}) and/or laser intensities (10^{16}–10^{17} W/cm^2) [3]. For higher densities ($\sim 10^{20}$ cm^{-3}), it was shown that the plasma temperature might reach 1 keV due to nonlinear inverse bremsstrahlung (IB) absorption and to stimulated Raman scattering [4]. Particle-in-cell (PIC) simulations—carried out for a moderate laser intensity ($I \approx 10^{17}$ W/cm^2)—show that the efficiency of such heating processes may be limited by using a short-pulse driving laser ($\tau \sim 50$ fs) [5]. However, to decrease the lasing wavelength that scales as Z^2 in the recombination schemes—where Z is the atomic number—and to achieve a large gain, it is of interest to use heavy elements—which in turn require increasing laser intensities to reach the desired charge state—and high plasma density. Recent calculations [6] have shown that a lasing effect with gain coefficient as high as 1000 cm^{-1}, may occur on the $n=2 \rightarrow n=1$ ($\lambda = 25$ Å) and $n=3 \rightarrow n=2$ ($\lambda = 134$ Å) transitions of H-like nitrogen in a low-temperature (<50 eV), high-density ($>10^{20}$ cm^{-3}) plasma produced by a 10-TW, 60-fs Ti:sapphire laser focused at intensities around 10^{19} W/cm^2. In this case, the ATI energy of the electrons released by H-like ions can reach several keV. The laser power can also exceed the critical power for relativistic self-focusing and electrons can be accelerated by the ponderomotive force and heated by parametric instabilities. The temperature then appears as a crucial issue for future prospects on transient recombination x-ray laser schemes in OFI produced plasmas.

In this paper, we report detailed space- and time-resolved electron density measurements on a plasma produced by optical-field ionization of a high-density (up to 10^{20} atoms/cm^3) nitrogen pulsed gas jet by an ultraintense ($I \approx 10^{19}$ W/cm^2) femtosecond ($\tau = 60$ fs) laser pulse using a Mach-Zehnder interferometer. The results were accurately modeled by a one-dimensional (1D) hydrodynamic code in cylindrical geometry, which allowed to infer the initial plasma temperature. This is, to our knowledge, the first time that such a study was carried out for this range of laser and gas target parameters.

The experiments were performed with the ultra high intensity (UHI10) laser that was designed to generate 10-TW ultrashort pulses with a 10-Hz repetition rate. It works according to the standard chirped-pulse-amplification technique. Titanium-sapphire rods are used as lasing medium and the operating wavelength of the system is 790 nm. In order to produce such high power ultrashort pulses with a good contrast, some specific optical systems had to be used. The low energy ultrashort pulse produced by a modified commercial Ti:sapphire oscillator is stretched up to 300 ps by an aberration-free Offner stretcher. After four amplification stages, the pulse energy is about 1.2 J (600 mJ after recompression). The pulse is then recompressed down to 60 fs in a vacuum chamber directly connected to the experimental chamber. The contrast, measured with a high-dynamics cross correlator is about 10^{-5} at 1 ps. The postpulse and prepulse amplitudes are less than 10^{-6}. The 80-mm diameter laser beam was focused with an $f/2.35$ off-axis parabolic mirror. The $1/e^2$ focal spot radius measured in vacuum was $w_0 = 8$ μm ($M^2 \sim 4$), giving a Rayleigh range of 70 μm and a peak intensity of 10^{19} W/cm^2. A small amount of the energy was picked up between the third and the fourth amplifier, and then sent to a second compressor. The pulse was recompressed in air down to 60 fs and had a 4-mJ energy after recompression. Its second harmonic provided a probe beam, perpendicular to the ionizing beam, for the Mach-Zehnder interferometer. The accuracy on the timing between the probe and the pump was limited by the pulse duration of the probe. The interferometry device supplied 2D maps of the electron density at different discret times up to 17 ns after the main pulse with a 60-fs time resolution. The spatial resolution in the object plane was 5 μm. The gas was delivered

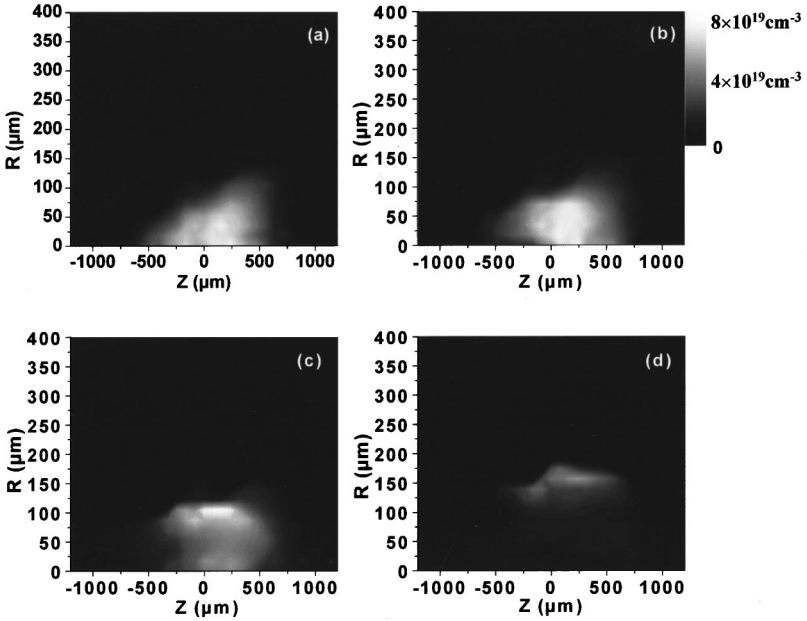

FIG. 1. The 2D maps of the plasma density measured, respectively, 16 (a), 200 (b), 970 ps (c), and 4.1 ns (d) after the laser pulse. The laser was propagated from the left to the right. The maximum density for $\Delta t = 16$ ps is 7.5×10^{19} cm^{-3}. The measurement is accurate to within $\pm 5\%$.

through a cylindrical nozzle with a 500-μm outlet. The density of atoms measured with the Mach-Zehnder interferometer has a Gaussian shape profile and decreases exponentially with the distance to the nozzle outlet. The laser was focused in the middle of the jet, 470 μm below the nozzle. Experiments were carried out for a 3.2-bar backing pressure. The density at the focus was 1.2×10^{19} atoms/cm^3, and the full width at half maximum of the Gaussian profile was 930 μm. The initial peak ionization stage of the plasma was deduced from the gas and electron density measurements well before the plasma expansion takes place. Time-integrated spectra of the x-rays ultraviolet (XUV) light emitted by the plasma were also recorded in the 2–20 nm wavelength range along the laser axis using a grazing-incidence flat-field spectrometer, providing a crossed measurement of the maximum ionization degree of the plasma.

Lines from H-like nitrogen were identified in XUV spectra. Therefore, if one expects that the plasma was created by OFI of the gas target, emission from H-like ions follows the recombination to bare nuclei, and the presence of H-like lines in the spectra indicates that a $Z_i = 7$ ionization stage was reached. The assumption of field ionization as the main ionization process is sustained by the observation that the intensity of H-like lines is very sensitive to laser power. For a 2-TW laser power, no emission from H-like ions is detected, and the peak ionization stage is only $Z_i = 5$. Moreover, previous spectroscopy measurements performed in the 1.88–1.96 nm wavelength range have demonstrated that fully stripped ions were produced for conditions close to those of the experiment described here [7].

The temporal evolution of the plasma was investigated with the Mach-Zehnder interferometer on a 17-ns time scale by delaying the probe with respect to the 10-TW ionizing beam. Figure 1 shows 2D maps in the position (r,z) of the electron density obtained by Abel inversion of the interferograms recorded, respectively, 16 (a), 200 (b), 970 (c), and 4.1 ns (d) after the ionizing pulse. The origin of time was defined with respect to the minimum shift that can be measured on the fringe pattern at the beginning of the jet. The laser propagated from the left to the right. The position $z = 0$, along the laser axis, corresponds to the position of the focus in vacuum. We verified that there was no plasma prior to the arrival of the 10-TW beam in the jet, and produced by the amplified spontaneous emission pedestal or by a prepulse. The plasma density at an early time ($\Delta t = 16$ ps) peaks at 7.5×10^{19} cm^{-3}. The ratio of the electron density at this time to the initial density of atoms gives a maximum ionization stage of $Z_i = 6.2 \pm 0.6$, in agreement with spectroscopy measurements. The density profile is nearly Gaussian along the two directions. Up to 200 ps after the laser pulse, the plasma radius increases but the density remains maximum on axis. After 970 ps, the plasma has expanded in the surrounding gas, a channel has formed, and a shock has developed. At this time, the channel density is about half the maximum density. For a 4.1-ns delay, the electron density on the channel axis is ten times smaller than the initial density and the shock is 150 μm away from the axis. No plasma expansion is observed along the z axis, as expected for a laser pulse much shorter than the hydrodynamics time scale [8]. In Fig. 2, we have plotted with open circles the position of the shock front as a function of time for $z = +215$ μm. The shock propagates in the surrounding gas with an initial velocity $v_s \approx 4 \times 10^6$ cm/s. About 300 ps after the ionizing pulse, the wave front radius fits a $t^{1/2}$ law, typical of a cylindrical blast wave propagation [9].

A detailed modeling of the plasma expansion was performed with the 1D Lagrangian hydrocode BREAKDOWN [10], in cylindrical geometry. The laser energy deposition was supposed to be instantaneous. Actually, it was a free parameter that was chosen in order to reproduce the initial experimental radial density profile and to fit the ionization stage. Ions and electrons were described by a perfect gas equation of state and heat conduction was calculated with the classical Spitzer-Härm formula with a flux limiter ($f = 0.1$). Ionization and recombination in the hydrocode were de-

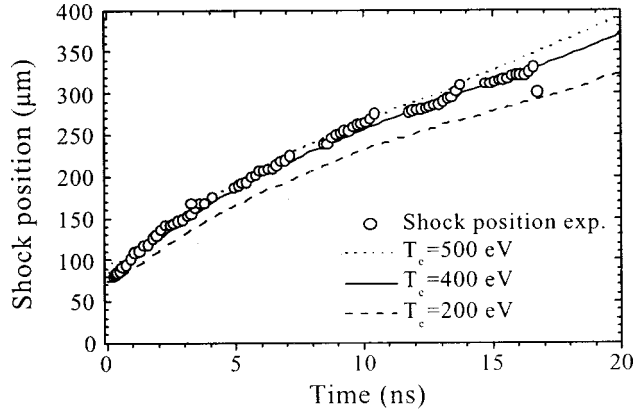

FIG. 2. Shock position versus time measured at $z=+215\ \mu$m (open circle) and calculated for $T_e=200$ (dashed line), 400 (solid line), and 500 eV (dotted line). The best fit of the data is obtained for $T_e=400$ eV.

scribed by a time-dependent collisional-radiative model by taking into account several energy levels for H-like, He-like, Li-like, and Be-like ions. For lower charge states, only the fundamental energy level was taken into account. The result of the calculations performed for an initial electron temperature of 200, 400, and 500 eV, respectively, is shown in Fig. 2.

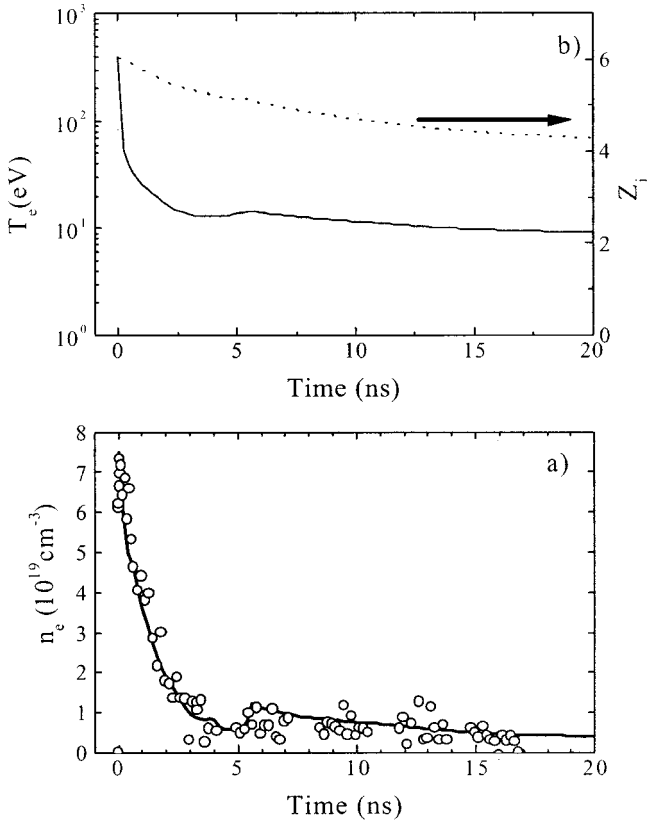

FIG. 3. (a) Time history of the density on the plasma axis ($r=0$) deduced from the interferometry measurements at $z=+215\ \mu$m (open circle) and given by the hydrocode for $T_e=400$ eV (solid line). (b) Time evolution of the temperature (solid line) and the ionization stage (dotted line) on axis as predicted by the code.

The best fit to the data was obtained for $T_e=400$ eV. The error bar on the initial temperature is $+/-50$ eV and is due to the experimental uncertainty on the position of the shock front. In Fig. 3(a), we have plotted the time history of the density on the plasma axis ($r=0$) deduced from the interferometry measurements at $z=+215\ \mu$m (open circle) and given by the hydrocode for $T_e=400$ eV (solid line) while Fig. 3(b) depicts the temporal evolution of the temperature (solid line) and the ionization stage (dotted line) on axis predicted by the code. One can note the very good agreement found between numerical and experimental results on the temporal evolution of the central density [Fig. 3(a)]. The predicted temperature, reported in Fig. 3(b), drops from 400 to 50 eV in about 200 ps and then decreases more slowly, reaching 15 eV in 2.4 ns while the electron density drops from 7.5×10^{19} to 6×10^{19} cm^{-3} on the first 200 ps and reaches 1.5×10^{19} cm^{-3} after 2.4 ns. The calculation shows that the plasma cooling is governed by the electron thermal conduction that smooths the density gradient at early times (<200 ps) and by the hydrodynamic expansion that generates a shock later on. This is in fairly good agreement with the experimental observations that show that the density channel formation and the shock development began more than 200 ps after the ionizing pulse. On the other hand, the evolution of the ionization stage given by the code indicates a very slow recombination with a predicted recombination time from H-like to He-like ion of 6.5 ns.

Electron heating cannot result here from IB absorption because the laser pulse duration is too short for electron-ion collisions to be effective. It can neither be due to the ionization process. The estimated residual ATI temperature was found to be only 45 eV [11]. In order to identify the mechanism responsible for the plasma heating, extensive 2D PIC calculations have been performed [6,12]. It has been found that the plasma is strongly heated by the high-intensity laser pulse due to stimulated Raman backscattering, and a 900-eV peak electron temperature has been predicted. This value is in qualitative agreement with the one deduced from the time evolution of the shock front.

Finally, in the perspective of studies on new x-ray laser schemes in optical-field ionized gases, we also addressed the

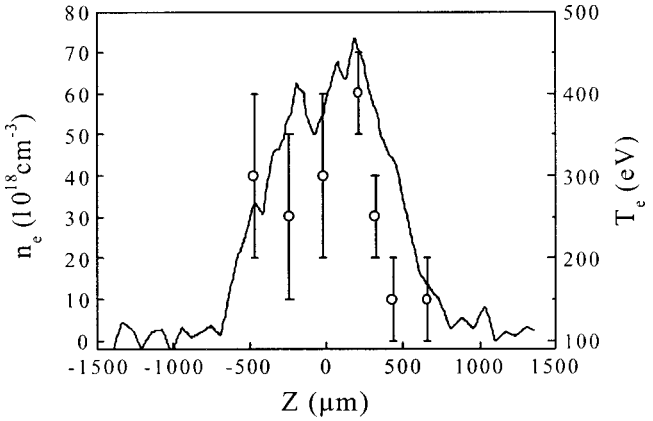

FIG. 4. On-axis longitudinal density profile measured at time $t=16$ ps (solid line) and initial temperature along the plasma axis as predicted by the hydrocode (open circle).

question of the homogeneity of the initial temperature along the plasma axis. The temperature profile was reconstructed from hydrocode simulations performed for different discrete positions along the *z* axis. This 1D treatment is valid as long as no longitunal plasma expansion takes place. This was verified on the experimental data by calculating the radial integral of the electron density for different discrete times. The integral was found to be constant as a function of time, which demonstrates that there is no plasma expansion along the *z* axis. Figure 4 gives the longitudinal electron density profile measured 16 ps after the laser pulse on the plasma axis (solid line) and the temperature profile inferred from hydrocode simulations (open circle). It is worth noting that the temperature is fairly uniform on about 700 μm, the variation remaining in the error bars, and then drops to 150 eV over 230 μm.

In summary, we have demonstrated that a plasma produced by OFI of a high-density (up to 10^{20} cm^{-2}) nitrogen gas jet by a short-pulse ($\tau = 60$ fs) high-intensity ($I \approx 10^{19}$ W/cm^2) laser is heated up to several hundred electronvolts during the interaction with the laser, and cools down due to thermal conduction and hydrodynamic expansion later on. Concerning future prospects on recombination x-ray laser schemes in OFI produced plasmas, this study shows that the initial temperature ($T_e \approx 400$ eV) is too high to observe a transient gain on transitions of H-like nitrogen. However, a lasing effect in the long lasting regime of recombination can still be achieved on the $n=3 \rightarrow n=2$ ($\lambda = 134$ Å) transition [6].

[1] Y. Nagata *et al.*, Phys. Rev. Lett. **71**, 3774 (1993); K. M. Krushelnick, W. Tighe, and S. Suckewer, J. Opt. Soc. Am. B **13**, 306 (1996).

[2] N. H. Burnett and G. D. Enright, IEEE J. Quantum Electron. **26**, 1797 (1990).

[3] A. A. Offenberger *et al.*, Phys. Rev. Lett. **71**, 3983 (1993); T. E. Glover *et al.*, *ibid.* **73**, 78 (1994); **75**, 445 (1995).

[4] W. Blyth *et al.*, Phys. Rev. Lett. **71**, 3983 (1993).

[5] P. Amendt, D. C. Eder, and S. C. Wilks, Phys. Rev. Lett. **66**, 2589 (1991).

[6] S. Hulin *et al.*, Phys. Rev. E **61**, 5693 (2000).

[7] F. B. Rosmej *et al.*, J. Phys. B **32**, L107 (1999).

[8] J. C. Griesemann and M. Decroisette, J. Appl. Phys. **50**, 3915 (1979); M. Dunne *et al.*, Phys. Rev. Lett. **72**, 1024 (1994); T. R. Clark and H. M. Milchberg, *ibid.* **78**, 2373 (1997).

[9] Ya. B. Zel'dovich and Yu P. Raizer, *Physics of Shock Waves and High Temperature Hydrodynamic Phenomena* (Academic, New York, 1966).

[10] M. J. Grout, K. A. Janulewicz, S. B. Healy, and G. J. Pert, Opt. Commun. **141**, 213 (1997).

[11] N. E. Andreev *et al.*, JETP Lett. **68**, 592 (1998) [Pis'ma Zh. Eksp. Teor. Fiz. **68**, 566 (1998)].

[12] P. Monot *et al.*, Phys. Plasmas **8**, 3766 (2001).